



A negative feedback bionic hydrogel reverses damaged cartilage microenvironment and induces targeted BMSCs differentiation for cartilage regeneration

Zhi Zheng, Jian Sun, Jun Wang, Suisui He, Yun Huang, Xu Yang, Yuqi Zhao, Cui-Yun Yu*, Hua Wei*

Hunan Province Cooperative Innovation Center for Molecular Target New Drug Study & School of Pharmaceutical Science, Hengyang Medical School, University of South China, 28 W Changsheng Road, Hengyang 421001, Hunan, China

ARTICLE INFO

Keywords:

Bionic hydrogel
BMSCs
Feedback regulation
Cartilage regeneration

ABSTRACT

The compromised microenvironment after cartilage injury generally leads to low survival or abnormal differentiation of implanted stem cells for fibrocartilage formation with weak mechanical properties. Suitable and safe bionic materials can provide mechanical properties for cartilage repair while promoting cartilage regeneration effects. However, to our knowledge, mechanical strength modulation of therapeutic peptide-based bionic hydrogels remains relatively unexplored, and further application of peptide-based bionic hydrogels in a negative feedback manner for defective cartilage repair has been seldom reported so far. In this study, we reported the first sophisticated design and fabrication of a dual cross-linked peptide-based hydrogel for promoted cartilage regeneration in a feedback-regulated manner. The integration of multiple supramolecular forces including host-guest interactions and extensive hydrogen bonding endow the resulting hydrogels with excellent self-healing and mechanical strength for highly synergistic lubrication properties and compressive performance. More importantly, the unique integrative peptide VPM-pmTGF- β 1 can realize on-demand pmTGF- β 1 release that is triggered by the MMP-3-responsive cleavage of a VPM sequence. When the VPM-pmTGF- β 1-modified hydrogel system is implanted into the cartilage defect sites in a model of SD rats, MMP-3-triggered on-demand pmTGF- β 1 release suppresses $\text{I}\kappa\text{B}\alpha/\text{NF-}\kappa\text{B}$ signaling pathway-induced cartilage inflammation in a negative feedback manner while promoting the targeted cartilage differentiation of BMSCs for efficient cartilage regeneration. The novel strategy developed herein contributes to a more comprehensive and in-depth understanding of the biological properties of peptide-based hydrogels for cartilage defect repair and provides a simple yet powerful means for clinical translations.

1. Introduction

Cartilage injuries are predicted to result in disability for over 350 million people worldwide by 2030 according to the World Health Organization report [1,2], accounting for a substantial burden on healthcare systems and patients. Articular cartilage defects are a common non-self-healing clinical orthopedic disease due to the absence of blood vessels, nerves and lymphatic tissue in the cartilage [3–6]. Despite stem cell-based therapies have shown significant potential for cartilage regeneration via cartilage differentiation and paracrine mechanisms, the inflammatory and oxidative stresses prevalent in the cartilage injury microenvironment result in low survival of implanted stem cells or abnormal differentiation into fibrocartilage with very weak mechanical proper-

ties [7–9]. Therefore, it is crucial to perform multidimensional regulation of the compromised joint microenvironment to promote cell survival and proliferation, as well as directed chondrogenic differentiation of stem cells to facilitate cartilage regeneration.

The development of a scaffold that can effectively remodel the damaged cartilage microenvironment and the normal differentiation of stem cells is a highly promising approach for stem cell-based cartilage repair. Recently, injectable hydrogels as a minimal invasive technology have attracted considerable attention [10–13]. Natural and synthetic polymers have been utilized to construct diverse injectable hydrogels with a favorable 3D microenvironment that can enhance the survival and retention of BMSCs within cartilage [14–17]. In addition to the 3D network required for basic biocompatibility and biodegradation, an

* Corresponding authors.

E-mail addresses: yucuiyunusc@hotmail.com (C.-Y. Yu), weih@usc.edu.cn (H. Wei).

<https://doi.org/10.1016/j.cej.2023.145228>

Received 13 June 2023; Received in revised form 26 July 2023; Accepted 3 August 2023
1385-8947/© 20XX

ideal hydrogel scaffold should have certain mechanical and self-healing properties that meet the requirements for cartilage repair because insufficient mechanical and self-healing properties led to hydrogel rupture after implantation without sufficient support and protection for the encapsulated cells [18,19]. The successful chondrogenesis of BMSCs requires not only strong physical support of cells by the hydrogel scaffold, but also sustained exposure of cells to factors that promote chondrogenesis.

Amino acids have been extensively recognized for numerous inherent advantages such as minimal immune rejection, ease of functionalization and degradation products for energy supply [20,21]. Gelatin, a polydisperse protein hydrolysed from collagen, provides adhesion sites for stem cells due to its arginine-glycine-aspartate (RGD) sequence [22–24]. γ -Polyglutamic acid (γ -PGA) is an amino acid multimer with amino groups, carbonyl groups and a large number of free carboxyl groups in the molecular structure, which provides excellent water retention and locking properties [25,26]. To design an injectable hydrogel system suitable for cartilage repair, we developed herein a dual crosslinked hydrogel scaffold based on gelatin and γ -PGA. The hydrogels were mainly constructed from carboxymethyl- β -cyclodextrin (CM- β -CD), *n*-hydroxy succinimide (NHS)-modified gelatin (β -CD-g-NHS), and adipic dihydrazide (ADH) and 1-adamantaneacetic acid (1-Ad)-modified γ -PGA (Ad- γ -PGA-ADH). That is, facile mixing β -CD-g-NHS and Ad- γ -PGA-ADH at room temperature leads to the formation of the physical crosslinked hydrogel network via supramolecular host-guest interactions between β -CD and Ad. Further formation of amide crosslinks between the amino groups of Ad- γ -PGA-ADH and NHS groups of β -CD-g-NHS serve as the chemical crosslinked hydrogel network. Note that the formation of large number of hydrogen bonding between the molecular chains of the hydrogels further endows the hydrogels with a reversible dynamic network together with the host/guest interactions. The developed hydrogel system thus has excellent mechanical properties, *i.e.*, the dynamic physical crosslinked network can be effectively de-crosslinked to dissipate energy under pressure, and quickly recovered by restoring the reversible crosslinking bonding upon pressure removal; meanwhile, the chemical crosslinked network ensures the structural integrity of the hydrogel for providing encapsulated cells and loaded therapeutic agents with strong support and interior network space [27–29].

Besides the inherent properties of the hydrogels required for cartilage repair, further physical encapsulation or chemical conjugation of bioactive species within the hydrogels is crucial for precise cartilage repair via on-demand release of the loaded cargoes for the exertion of therapeutic effects. M1 macrophages release large amounts of inflammatory factors such as TGF- α , IL-1 β , and IL-6 after cartilage damage, which disrupts the metabolic balance of chondrocytes and triggers the inflammatory response [30,31]. These inflammatory factors bind to specific receptors on the chondrocyte membrane, activating the I κ B α /NF- κ B signaling pathway and causing the release of large amounts of inducible nitric oxide synthase (iNOS), cyclooxygenase-2 (COX-2) and matrix metalloproteinases (MMPs) from chondrocytes [30,32]. Among the released MMPs, MMP-3 is highly expressed in early-stage injured cartilage and plays a critical role in cartilage degradation by directly breaking down cartilage extracellular matrix (ECM) components and activating several other pro-MMPs [33–35]. Therefore, inhibiting the release of inflammatory factors from early macrophages may be an effective strategy to prevent matrix degradation in damaged cartilage and minimize patient pain.

Considering the aforementioned inflammation and stem cell transplantation issues after cartilage injury, we integrated a peptide sequence composed of VPMSMRGG (VPM), an MMP-3 cleavable peptide sequence and ACESPLK(R)QCGGGS (pmTGF- β 1), a transforming growth factor- β 1 (TGF- β 1) mimetic peptide for cartilage defect repair [30,36]. The VPM sequence with sensitivity to MMP-3 protein hydrolysis acts as an MMP-3 inhibitor peptide [36], while the pmTGF- β 1 mimetic peptide

has a similar function to TGF- β 1 in inhibiting inflammation and promoting cartilage differentiation [30,37,38]. The two sequences are linked via a stable covalent bond to produce a double peptide-linked VPM-pmTGF- β 1 sequence capable of responding to MMP-3 cleavage for pmTGF- β 1 releases. The N-terminal amino group of VPM-pmTGF- β 1 were finally chemical grafted to β -CD-g-NHS to yield a VPM-pmTGF- β 1-functionalized hydrogel system. When the VPM-pmTGF- β 1-modified hydrogel system is implanted into the sites of cartilage defects, MMP-3-triggered on-demand pmTGF- β 1 release suppresses I κ B α /NF- κ B signaling pathway-induced cartilage degeneration in a negative feedback manner while promoting the targeted cartilage differentiation of BMSCs and efficient cartilage regeneration (Scheme 1). Comprehensive *in vitro* and *in vivo* evaluations were performed to demonstrate the effectiveness of this peptide-conjugated dual crosslinked hydrogels in cartilage repair.

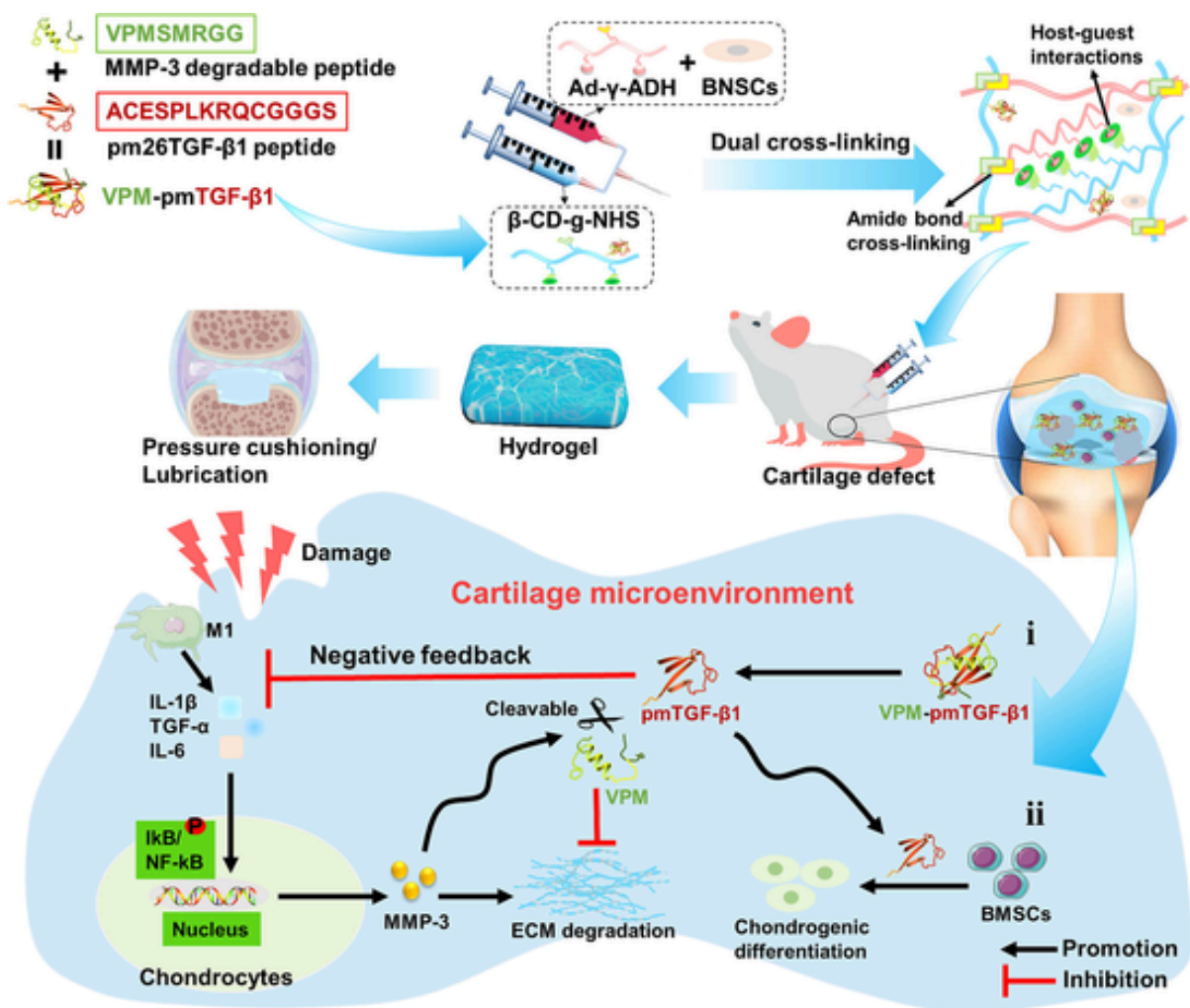
2. Materials and method

2.1. Materials

Type A gelatin from porcine skin (CAS: 9000–70-8) was supplied by Sigma-Aldrich (St. Louis, USA). Adipic dihydrazide (ADH, CAS: 1071–93-8), γ -polyglutamic acid (γ -PGA, CAS: 25513–46-6), *N*-hydroxysuccinimide (NHS, CAS: 6066–82-6), Carboxymethylated- β -cyclodextrin (CM- β -CD, CAS:218269–34-2), 1-Adamantaneacetic acid (1-Ad, CAS: 4942–47-6), and 1-Ethyl-3-(3-dimethylaminopropyl) carbodiimide hydrochloride (EDC-HCl, CAS: 25952–53-8) were purchased from Aladdin Industrial, Inc. (Shanghai, China). Anti-aggrecan (Cat No: ab3773), anti-Col II (Cat No: ab34712), anti-NF- κ B (Cat No: ab16502), anti-NF- κ B p65 (Cat No: phospho S536 ab76302), anti-MMP-3 (Cat No: ab52915), anti-TGF- α (Cat No: ab227723), anti-IL-1 β (Cat No: ab254360), recombinant MMP-3 protein (Cat No: ab96555), and MMP-3 ELISA (Cat No: ab270216) kit were purchased from Abcam (Cambridge, USA). Anti-CD86 (Cat No: 13395–1-AP), anti-CD206 (Cat No: 18704–1-AP), IL-1 β ELISA kit (Cat No: KE20021), Phalloidin (Cat No: PF00003), IL-1 β standard (Cat No: HZ-1164), and TGF- β 1 standard (Cat No: HZ-1011) were purchased from Proteintech (Chicago, USA). UK 356618 (Cat No: HY-107394) was purchased from MedChemExpress (New Jersey, USA). ACESPLK(Ac)RQCGGGS (pmTGF- β 1), VPMSMRGG-ACESPLK(Ac)RQCGGGS (VPM-pmTGF- β 1), and VPM-pmTGF- β 1-FITC were purchased from GL Biochem Ltd. (Shanghai, China). BMSCs were kindly provided by the Cell Bank of the Chinese Academy of Sciences. Cell culture medium and fetal bovine serum (FBS) were purchased from Gibco (USA). All chemical and biological reagents were commercially available and were used as received, unless otherwise stated.

2.2. Preparation and characterization of β -CD-g-NHS

Briefly, 0.5 g of CM- β -CD was dissolved in 100 mL of ultrapure water and stirred well at 40°C. Then, 1.5 mmol of NHS and 1.5 mmol of EDC were added to activate the carboxyl groups on the CM- β -CD for 2 h. Finally, 1 g of gelatin was dissolved in 50 mL of ultrapure water, slowly dropped into the CM- β -CD solution, and reacted for 24 h at pH 4–5. At the end of the reaction, the solution was dialyzed (8000–14000 MWCO) and the β -CD-gelatin was harvested by freeze-drying. For the synthesis of β -CD-g-NHS, 0.5 g of β -CD-gelatin was dissolved in 16 mL of ultrapure water, stirred well and activated with 16 mmol of EDC for 1 h. Then, 16 mmol of NHS was added to the CM- β -gelatin solution and allowed to react for 24 h. The solution was dialyzed (8000–14000 MWCO) for more than 3 days. The precipitate was removed by centrifugation, freeze-dried and structurally characterized by ¹H NMR and FT-IR for β -CD-gelatin and β -CD-g-NHS.



Scheme 1. Schematic illustration of a peptide-based hydrogel with multifunctional properties for cartilage regeneration.

2.3. Preparation and characterization of Ad-γ-PGA-ADH

Briefly, 2 g of γ -PGA was dissolved in 200 mL of ultrapure water, and then 7.5 mmol of NHS and 7.5 mmol of EDC were added to the solution and allowed to react for 1 h. Finally, 2.5 g of ADH was added to the reaction solution at pH \sim 5.5 for 24 h. The reaction solution was dialyzed (8000 MWCO) for at least 3 days, and the product was freeze-dried. For the synthesis of Ad- γ -PGA-ADH, 0.24 g of 1-adamantaneacetic acid was dissolved in 100 mL of water/DMSO (1:3), and 1.5 mmol of EDC and 1.5 mmol of NHS were added to this mixture and stirred for 6 h at room temperature. 1 g of γ -PGA-NH₂ dissolved in 100 mL of ultrapure water was dropped into 1-adamantaneacetic acid solution and allowed to react for 40 h at room temperature. The reaction solution was centrifuged to remove the precipitate, dialyzed (8000 MWCO) for at least 3 days, and freeze-dried, and then the structures of γ -PGA-ADH and Ad- γ -PGA-ADH were characterized by ¹H NMR and FT-IR.

2.4. Peptide covalently coupled β -CD-g-NHS

To maintain consistent in vitro and in vivo hydrogel properties, 15% NHS-functionalized β -CD-gelatin was used for characterization, while 22% NHS-functionalized β -CD-gelatin was used for cellular and animal studies (7.2% of the NHS was consumed by the peptide). Briefly, 10 mg of peptide was added to 1 wt% β -CD-g-NHS and allowed to react for 5 h at 4 °C to consume the NHS groups. The solution was subsequently

titrated to neutral pH with 5 N NaOH, dialyzed with cold ultrapure water, and lyophilized to obtain peptide covalently coupled β -CD-g-NHS. Verification of the reduction in the NHS peak and the presence of the characteristic peak of the conjugated peptide for peptide-loaded β -CD-g-NHS was carried out using ¹H NMR.

2.5. Testing of hydrogel mechanical properties

The storage modulus (G') and loss modulus (G'') of the hydrogel cylindrical samples (diameter = 1 cm, height = 1 cm) were detected using a rotational rheometer (Malvern, UK). Time sweep tests were performed in the time range of 0–20 min, and frequency sweep tests were performed in the frequency range of 0.1–10 Hz to obtain the final G' and G'' for each hydrogel sample. The stress-strain curve for each hydrogel sample was obtained by placing a cylindrical sample in a universal material testing machine (INSTRON 3365) and performing compression tests at a rate of 0.5 mm/min.

2.6. Swellability and degradability of hydrogels

Briefly, Cylindrical hydrogel samples with a diameter and height of 1 cm were subjected to lyophilization, and their weights were recorded. The freeze-dried hydrogel samples were immersed in simulated body fluid (SBF) at 37 °C, from which samples were periodically removed and freeze-dried, and the weight was recorded. The degradation cycle of the hydrogels was finally obtained from the ratio of the mass lost to

the total mass. In addition, to investigate the structural stability of the hydrogels, different samples were immersed in SBF to mimic a physiological environment. Briefly, the hydrogels were placed in SBF at a concentration of 0.1 g/mL, incubated at 37 °C for 5 days, and then weighed again. The swelling rate of the hydrogel was derived from the change in weight before and after soaking.

2.7. Cell isolation and culture

Cartilage tissue was isolated from the joints of four-week-old SD rats, cut into pieces smaller than 1 mm³ and washed twice with antibiotic-containing PBS solution. The cartilage was placed in a centrifuge tube with 3 volumes of 0.25% trypsin and digested for 20 min. The supernatant was then discarded, and 0.2% collagenase II was added to digest the cartilage for 30 min. The digestion was terminated by adding serum-containing medium, and the digest was centrifuged at 1200 rpm for 8 min. The cells were resuspended in DMEM complete medium and incubated at 37 °C in a 5% CO₂ culture incubator.

2.8. BMSC chondrogenic differentiation assay

BMSCs were cultured in 15 mL centrifuge tubes containing chondrogenic medium. The medium was replaced every 2 days with fresh medium and peptide-loaded hydrogel precursor solution (2 μL) for 3 weeks. The resulting cell pellets were subsequently frozen and sectioned at 5 μm thickness for Alcian blue, Safranin-O staining, and H&E staining. In addition, BMSCs were cultured for 1 week in chondrogenic medium containing a peptide-loaded hydrogel precursor solution. Western blotting and immunofluorescence staining were performed to determine cartilage-related indices.

2.9. In vitro hydrogel biocompatibility assay

The β-CD-g-NHS/Ad-γ-PGA-ADH hydrogel precursor solution was added to in 96-well plates (100 μL/well) and placed in an incubator to form gels. BMSCs were then inoculated onto the gel surface of 96-well plates and placed in a 37 °C, 5% CO₂ incubator with periodic changes of fresh medium. To assess cell viability, BMSCs were loaded onto hydrogels using Calcein-AM and PI staining according to the kit protocol (Solarbio, China) and incubated in the incubator for 30 min. At the end of the incubation, the gels were washed with PBS, and the survival or proliferation of the BMSCs was observed using a laser confocal microscope (Nikon A1R); live cells stained with Calcein-AM were observed in green at 490 nm, and dead cells stained with PI were observed in red at 545 nm.

2.10. Peptide response release assay

The efficiency of MMP-3 inhibition was determined using a rat MMP-3 ELISA kit. Briefly, a mixture of VPM-pmTGF-β1 hydrogel extract containing rMMP-3 was dissolved in 100 μL of buffer and then added to a 96-well plate precoated with MMP-3-specific monoclonal antibody. Next, the mixture was incubated for 90 min at 37 °C in darkness. Finally, the fluorescence intensity of each sample endpoint was detected at a wavelength of 450 nm using a microplate reader (Perkin Elmer VICTORTM X4). The concentration of rMMP-3 was varied (1 ng/mL, 25 ng/mL, 50 ng/mL, 75 ng/mL, and 100 ng/mL) to detect the MMP-3 inhibition efficiency of the VPM-pmTGF-β1 hydrogel (50 μL).

FITC-labelled pmTGF-β1 was used to detect response release in hydrogels. Peptide-loaded hydrogels were added to in 48-well plates (50 μL per well, n = 4), followed by 100 μL of PBS and/or rMMP-3 (25 ng/mL), and incubated at 37 °C for 14 days. The dose-dependent release of pmTGF-β1 to MMP-3 was demonstrated in the presence of rMMP-3 (25 ng/mL) using different concentrations of the MMP-3 inhibitor UK356618 (1 nM, 5 nM, and 10 nM). The supernatant was col-

lected and centrifuged at 15000 rpm for 5 min at 4 °C, and the 517 nm fluorescence of supernatant FITC-pmTGF-β1 under 480 nm excitation was measured using a plate reader. The cumulative percentage of peptides released from the grafted material was calculated by comparison with the established standard curve.

2.11. Detection of chondrocyte inflammation

To simulate the inflammatory state of cartilage in vitro, chondrocytes were inoculated into 12-well plates and incubated with IL-1β (10 ng/mL) for 12 h. After washing with PBS, the medium was replaced with normal growth medium and treated with TGF-β1 (10 ng/mL) or VPM-pmTGF-β1 hydrogel precursor solution (50 μL) for 24 h. Immunofluorescence staining was performed to detect nuclear translocation of NF-κB in the cells. Inflammation-related factors and pathway protein expression were detected using immunofluorescence and western blot.

2.12. In vivo animal experiments

Sixty male SD rats (250 ± 30 g) were purchased from HUNAN SJA LABORATORY ANIMAL CO., LTD (Hunan, China). SD rats were used to create full-thickness cartilage defects to assess the cartilage regenerative capacity of the hydrogel. Briefly, rats were anaesthetized with sodium pentobarbital (3%, 30 mg/kg). A 2 mm diameter and 1.5 mm thick cartilage defect was created in the central region of the trochlear groove in the right leg of each rat. A pre-prepared hydrogel was then injected into the damaged cartilage. The SD rats were divided into six groups: the normal group, saline group, blank hydrogel group (50 μL), VPM-pmTGF-β1 hydrogel group, BMSCs/hydrogel group (1 × 10⁶ cells/50 μL), and BMSCs/VPM-pmTGF-β1 hydrogel group (1 × 10⁶ cells/50 μL). All animals were euthanized at 6 or 12 weeks after surgery, and knee joints were harvested for further analysis. All experimental designs and protocols involving animals were approved by the Experimental Animal Ethics Committee of the University of South China, Hunan, People's Republic of China (approval 4304079008946) and complied with the National Institutes of Health and University of South China guidelines on the care and use of animals for scientific purposes.

2.13. In vivo cartilage Regeneration-Related indicator assay

Western blotting was performed to detect the expression of chondrogenesis-related proteins (MMP-3, TGF-α, and IL-1β) in all treatment groups. After surgery, cartilage tissue and synovial tissue were separated and frozen in liquid nitrogen. These tissues were then milled with a mortar mixer to extract the proteins. To study the expression levels of inflammatory factors and MMP-3, proteins were electrophoresed, transferred to membranes, incubated with primary and secondary antibodies and visualized by a chemiluminescent imaging system. Additionally, immunofluorescence and immunohistochemical staining were employed, following the instructions provided with the respective antibodies, to detect the expression levels of relevant inflammatory factors and proteins in synovial tissues.

2.14. Histological analysis

After surgery, all rats were euthanized, and the cartilage was removed, fixed in 4% paraformaldehyde, decalcified in ethylenediaminetetraacetic acid and embedded in paraffin. H&E, Toluidine Blue, SO/Fast Green, and Col-II staining were used to detect neochondrogenesis and type II collagen expression. The repaired articular cartilage was assessed according to the International Cartilage Repair Society (ICRS) visual histological assessment criteria. In addition, blood was collected from each group of rats at the end of the treatment for

toxicological studies. One part of the blood was used for whole blood analysis and blood chemistry tests, and the other part was used for serum chemistry analysis. Blood biochemical and haematological analyses were performed at Servicebio Technology Ltd. (Wuhan, China).

2.15. Statistical analysis

All data were expressed as the mean \pm standard deviation and analyzed by one-way ANOVA of means between multiple groups. Statistical significance was * $P < 0.05$, ** $P < 0.01$, and *** $P < 0.001$.

3. Results and discussion

3.1. Fabrication of the β -CD-g-NHS/Ad- γ -ADH hydrogels

Cartilage is a smooth and flexible tissue that covers the bone surface in joints and plays the functions of cushioning and shock absorption [39–41]. To maximize the suitability of injectable hydrogels for cartilage tissue, the physicochemical properties of gelatin and γ -PGA were optimized via proper chemical modifications to enable their use as building moieties for construction of hydrogels with high modulus values and self-healing properties. A schematic illustration of the β -CD-g-NHS/Ad- γ -ADH hydrogel preparation is shown in Fig. 1A. First, the successful synthesis of β -CD-g-NHS was confirmed by the presence of characteristic signals of both β -CD and NHS in the ^1H NMR and FT-IR spectra of β -CD-g-NHS (Fig. 1B and Fig. S1–S3). The MMP-3 cleavage peptide VPM was prepared using a classical solid-phase peptide synthesis

technique and further combined with the pmTGF- β 1 peptide sequence to generate a VPM-pmTGF- β 1 composite peptide that was further conjugated to β -CD-g-NHS via an amidation reaction between the terminal amino group of the combinatorial peptide and NHS functions of β -CD-g-NHS under mild conditions. The successful synthesis of the combined peptide with a desired sequence and high purity was confirmed by mass spectrometry (MS) and HPLC analysis (Fig. S4 and S5). The total amounts of primary amino groups in gelatin and β -CD-gelatin were quantified using the 2,4,6-trinitrobenzenesulphonic acid (TNBSA) method, and the grafting density of β -CD onto gelatin was determined to be approximately 12.6%. Successful VPM or VPM-pmTGF- β 1 peptide conjugation to β -CD-g-NHS led to the consumption of NHS groups and the introduction of peptide characteristic peaks, which was supported by the ^1H NMR spectra of β -CD-g-peptide (Fig. S6 and S7). The peptide conjugation efficiency was calculated to be approximately 7.2%.

γ -PGA possesses extremely outstanding adhesive and moisturizing properties 2–3 times stronger than those of hyaluronic acid (HA) [25], which makes γ -PGA a highly promising candidate for dynamic surface attachment of cartilage tissue and stem cell loading. To enhance the mechanical and self-healing properties of gelatin, adipic dihydrazide (ADH) and 1-adamantaneacetic acid (1-Ad)-modified γ -PGA (Ad- γ -ADH) were synthesized in a two-step procedure (Fig. S1B). Ad- γ -ADH showed characteristic resonance signals at 1.76–1.85 ppm and 1.54 ppm attributed to the proton vibration of 1-Ad and $-\text{CH}_2-$ group of ADH, respectively in the ^1H NMR spectra (Fig. 1B and S8) and characteristic absorption bands of the amide group at 3100 cm^{-1} and 1531.5 cm^{-1} (Fig. S9) in the FT-IR spectrum. The grafting efficiency of 1-Ad to γ -PGA was determined by ^1H NMR analysis to be approximately

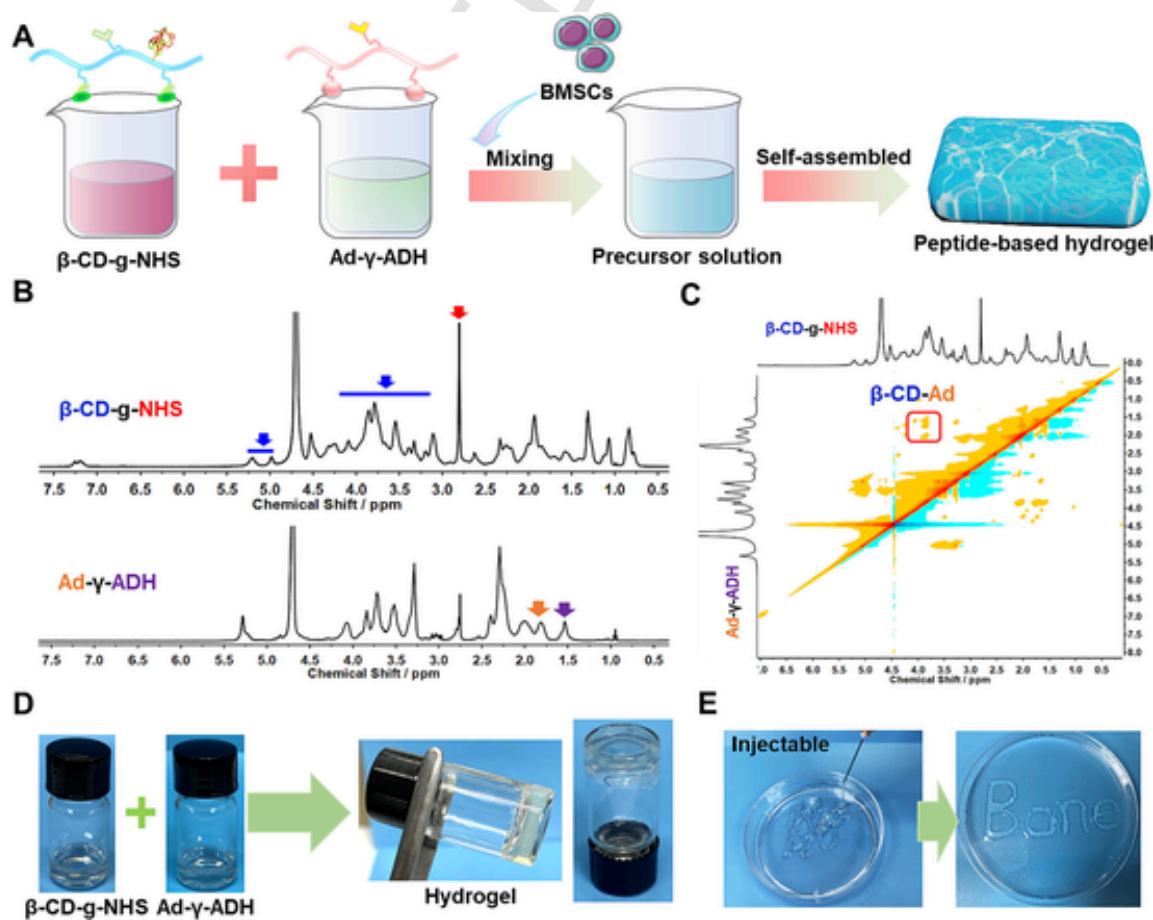


Fig. 1. Preparation of the β -CD-g-NHS/Ad- γ -ADH hydrogels. (A) Schematic diagram of the preparation of the β -CD-g-NHS/Ad- γ -ADH hydrogel. (B) ^1H NMR spectra of β -CD-g-NHS and Ad- γ -ADH. (C) NOESY patterns of the inclusion complexes of β -CD and Ad in the hydrogel in D_2O . (D) Photograph of the β -CD-g-NHS/Ad- γ -ADH hydrogel transition from solution to gel state. (E) Injectability of the β -CD-g-NHS/Ad- γ -ADH hydrogels.

11.3%. The successful occurrence of supramolecular β -CD/Ad host-guest interactions between β -CD-g-NHS and Ad- γ -ADH was evidenced by the appearance of cross peaks attributed to the interactions between the aromatic ring of Ad and the H3 proton inside the cavity of β -CD in the nuclear 2D overhauser effect spectroscopy (NOESY) spectra (Fig. 1C).

Finally, β -CD-g-NHS and Ad- γ -ADH solutions were mixed with an optimized feed ratio in a centrifuge tube to afford the rapid formation of a dual crosslinked hydrogels at 37 °C (Fig. 1D). The mixed hydrogel precursor solution could be smoothly passed through a 28-gauge needle syringe for subsequent injection into cartilage tissue (Fig. 1E).

3.2. Characterization of the β -CD-g-NHS/Ad- γ -ADH hydrogels

Gelation time is a critical factor in determining the efficacy of injectable hydrogels for cartilage repair. An ideal gelation time ensures easy control of an injection process and stable properties of the hydrogel during its lifetime once the gelation process is complete. The gela-

tion time for hydrogel formation was determined using a tube inversion method at 37 °C, which revealed a gelation time of approximately 40 s for the hydrogel precursor solution with a mixed composition of 25% β -CD-g-NHS and 4% Ad- γ -ADH (Fig. 2A). Although another composition, 30% β -CD-g-NHS/5% Ad- γ -ADH, exhibited a shorter gelation time, the mixed hydrogel precursor solution contained too many undissolved solids that is unbeneficial for injection. Scanning electron microscopy (SEM) observations of the 25% β -CD-g-NHS/4% Ad- γ -ADH hydrogel showed clearly microporous structures with an average pore size of approximately 50 μ m within the hydrogels (Fig. 2B), which promotes the proliferation and migration of BMSCs for cartilage repair.

Next, the rheological and mechanical properties of the β -CD-g-NHS/Ad- γ -ADH hydrogels were investigated by rotational rheometry. The storage modulus (G') and loss modulus (G'') were determined within 20 min in a time scan mode (Fig. 2C). The hydrogel modulus showed a dramatic increased trend following gradual elevated ratios of β -CD-g-NHS and Ad- γ -ADH units, up to a maximum modulus of 700 Pa. Moreover, G' was consistently larger than G'' at frequencies in a range of

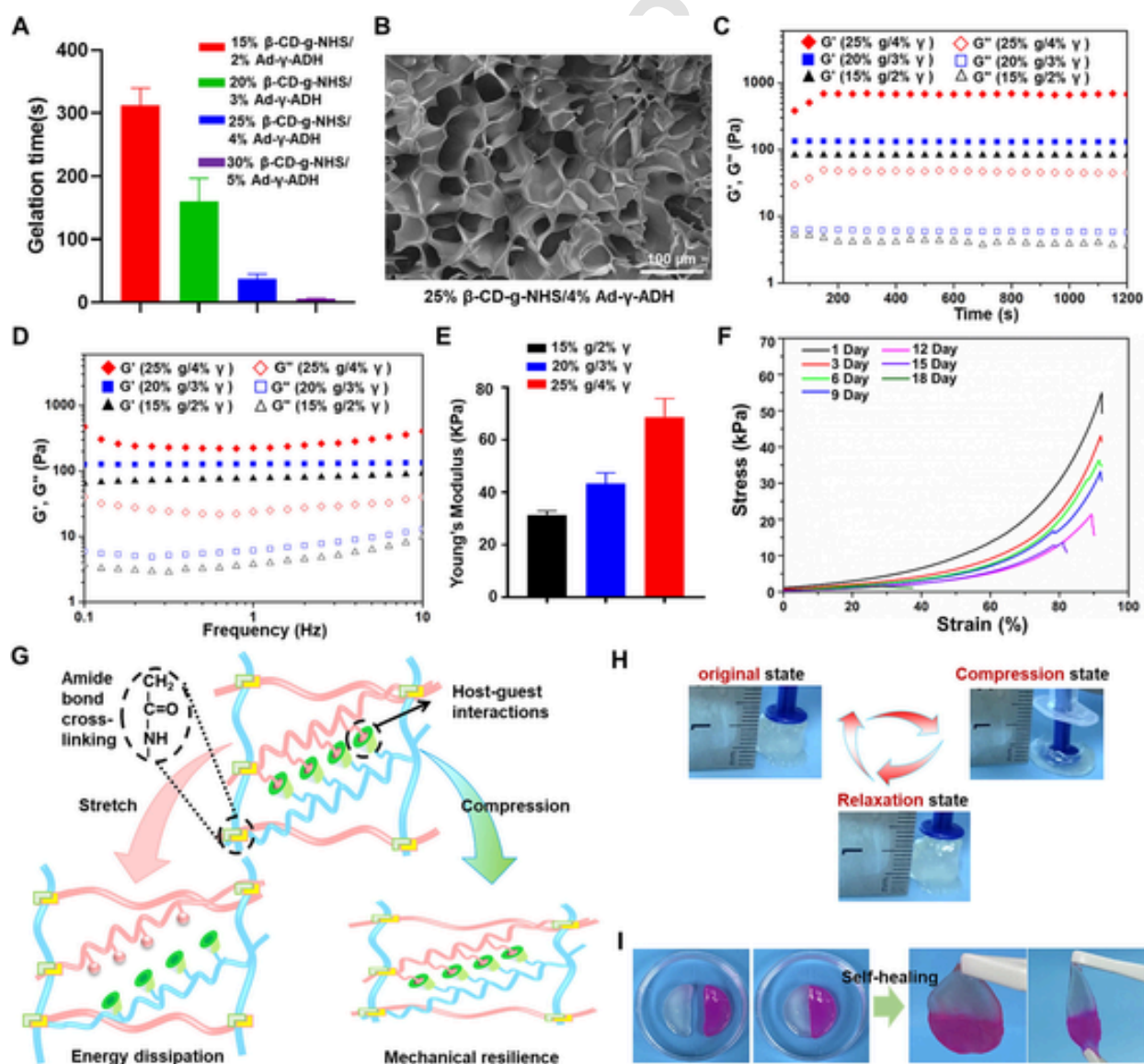


Fig. 2. Characterization of the β -CD-g-NHS/Ad- γ -ADH hydrogels. (A) Gelation time of the hydrogel samples. (B) SEM images of the 25% β -CD-g-NHS/4% Ad- γ -ADH hydrogel. (C) Rheological properties of hydrogel samples in time-scan mode. (D) Rheological properties of hydrogel samples in frequency sweep mode. (E) Young's moduli of the hydrogel samples ($n = 4$). (F) Stress-strain curve of the hydrogels in SBF medium for 20 days. (G) Schematic illustration of the mechanism of double crosslinked hydrogels formed by β -CD-g-NHS and Ad- γ -ADH. (H) Photographs of the β -CD-g-NHS/Ad- γ -ADH hydrogel in the original, compressed and relaxed states. (I) The self-healing process of the β -CD-g-NHS/Ad- γ -ADH hydrogels.

0.1 and 10 Hz, indicating that all the textured hydrogel samples had a morphology similar to that of an elastic solid (Fig. 2D). SEM measurements of the different hydrogel samples also confirmed that the 25% β -CD-g-NHS/4% Ad- γ -ADH hydrogel had a pore dimension smaller than those of the hydrogels prepared at the other ratios (Fig. S10). Stress-strain tests were performed on three hydrogel samples using a universal material testing apparatus (Fig. S11). The 25% β -CD-g-NHS/4% Ad- γ -ADH hydrogels exhibited the highest Young's modulus of ~ 70 kPa among all the groups (Fig. 2E).

The mechanical strength changes of the 25% β -CD-g-NHS/4% Ad- γ -ADH hydrogels were investigated by monitoring the mechanical properties of a cylindrical hydrogel with a diameter and a height of both 1 cm that was incubated in SBF medium for 20 days. As expected, the hydrogel exhibited time-dependent gradually decreased mechanical strength values due to the degradation in SBF. The hydrogel underwent a significant mass decrease greater than 30% for losing the ability to maintain the fixed original shape by the end of day 20, which thus prevented further mechanical property examination on a universal material testing machine. Such partially hydrogel degradation in SBF did not actually affect the performance of the hydrogel in cartilage repair applications because there is a lack of large amounts of articular synovial fluids in the cartilage cavity to immerse completely the hydrogel for prompt degradation, which ensures somewhat maintained mechanical properties of the hydrogels for a prolonged lifetime that can meet the effective disease treatment requirement. In addition, *in vitro* data demonstrated that the hydrogel could maintain a stable structure in a two-week duration that corresponds to the early stage of cartilage damage, suggesting that the hydrogel-mediated on-demand release of anti-inflammatory factors in response to the early abundant MMP-3 guarantees the exertion of bio-functions for enhanced treatment efficiency (Fig. 2F).

Next, the cylindrical hydrogel composed of 15% β -CD-g-NHS and 2% Ad- γ -ADH degraded $\sim 80\%$ in simulated body fluid (SBF) within 20 days, while the 25% β -CD-g-NHS/4% Ad- γ -ADH hydrogel degraded $\sim 30\%$ in SBF due to the dense structure (Fig. S12), showing a relatively stable degradation cycle. In a swelling ratio test, all the hydrogel samples reached swelling equilibrium after 24 h of immersion in SBF. The 25% β -CD-g-NHS/4% Ad- γ -ADH hydrogel showed a swelling ratio of 15% lower than those of the other hydrogel samples. A low swelling ratio contributed to the maintenance of the original hydrogel shape with stabilized mechanical properties *in vivo* (Fig. S13). As a result, the 25% β -CD-g-NHS/4% Ad- γ -ADH hydrogel was screened for the subsequent cartilage defect study in terms of its better properties than those of the other hydrogel samples.

The reversible self-healing properties of hydrogels play a critical role in cartilage repair, as cartilage tissue undergoes constant mechanical stress and needs to withstand the corresponding mechanical cycles to prevent any burst release of the encapsulated therapeutic agents [42]. The dual crosslinked hydrogel combines the biological advantages of gelatin and γ -PGA with excellent mechanical properties. The strong chemical network composed of covalent amide bonds can maintain the hydrogel intactness in compression-stretch tests, meanwhile the physical network consisting of dynamic host-guest interactions and extensive hydrogen bonding network guarantees prompt recovery of the hydrogel to its original structure upon pressure removal (Fig. 2G). The dual crosslinked hydrogel can withstand over 90% deformation and get complete recovery upon pressure removal, supporting its excellent elastic properties (Fig. 2H). The excellent self-healing properties of the hydrogel were evidenced by the formation of stretchable intact hydrogels in a short time via inter-adhesion of the rhodamine-stained gels (Fig. 2I). It is worth pointing out that the availability of large amount of hydrogen bonding makes the hydrogel highly adhesive to various materials, thus its enhanced adhesion to damaged cartilage tissue without any undesired displacement (Fig. S14). Overall, an elegant integration of these dual networks enables the hydrogels with modulated mechani-

cal strength and excellent self-healing properties for lubrication and cushioning cartilage tissue pressure.

3.3. *In vitro* response release studies of peptides

As a peptide mimic to TGF- β 1, pmTGF- β 1 has similar effects in promoting cartilage differentiation and suppressing inflammation [30,37,38]. Peptides physically encapsulated in a hydrogel may exhibit a premature burst release at the injury site with compromised therapeutic effects [5,17]. To achieve controlled and sustained peptide release at the injury site, pmTGF- β 1 was covalently conjugated to the hydrogel polymer chain via a sensitive linker. Specifically, an MMP-3 cleavable peptide, VPMSMRGG (VPM) was placed between β -CD-g-NHS and pmTGF- β 1 to achieve on-demand pmTGF- β 1 release. The MMP-3 concentration in the synovial fluid of rat cartilage has been reported to be in a range of 1–100 ng/mL, dependent on the severity of the injury [33,43,44]. The upregulated expression of MMP-3 starts 1 h after cartilage injury and lasts for more than 3 weeks [45,46]. Therefore, reducing excessive MMP-3 accumulation at the cartilage injury site is considered one of the main therapeutic targets to inhibit early ECM degradation. Upon injection of the peptide-loaded hydrogels into the injured cartilage site, gradual consumption of VPM peptide sequence by upregulated MMP-3 leads to on-demand pmTGF- β 1 release for the exertion of dual functions, *i.e.*, inhibiting inflammation and promoting chondrocyte differentiation (Fig. 3A).

Since VPM, a peptide sequence with a protein binding site could be generally degraded or cleaved upon contact with a specific substrate protein [36], our initial design involved the use of a recombinant MMP-3 (rMMP-3) protein and an effective MMP-3 inhibitor, UK356618, to explore the effect of MMP-3 responsiveness on the VPM-pmTGF- β 1 hydrogels. The results clearly demonstrated significantly reduced activities of rMMP-3 only in the hydrogel formulation containing the VPM sequence (Fig. 3B), because rMMP-3 can cleave the VPM sequence in the VPM-pmTGF- β 1 hydrogel for MMP-3 consumption and subsequent pmTGF- β 1 release. To further determine the saturation level of MMP-3 when using 50 μ L (a dose for subsequent cartilage repair) of VPM-pmTGF- β 1 hydrogel, different doses of MMP-3 were administrated to assess the saturation effect on the VPM peptide. A saturation tendency at approximately 50 ng/mL to 70 ng/mL of MMP-3 was thus identified (Fig. 3C), suggesting that 50 μ L of VPM-pmTGF- β 1 hydrogel could completely deplete 50 ng/mL of MMP-3 to release an equivalent proportion of pmTGF- β 1. Finally, we directly examined the on-demand pmTGF- β 1 release from the hydrogel using two methods. We first investigated the time-dependent cumulative pmTGF- β 1 release from the hydrogel at a dose of 50 ng/mL of rMMP-3. The cumulative pmTGF- β 1 release was minimal in the presence of only PBS or UK356618, whereas incubation with a periodic added MMP-3 led to significantly greater cumulative pmTGF- β 1 release, supporting an MMP-3-responsive on-demand pmTGF- β 1 release profile for the hydrogels (Fig. 3D). To identify clearly whether the accelerated cumulative pmTGF- β 1 release was attributed to the hydrogel degradation or other factors, we further examined the pmTGF- β 1 release properties by a competition study, *i.e.*, in the presence or absence of UK356618 on day 3. The release rate of pmTGF- β 1 from MMP-3-incubated hydrogels decreased significantly with increasing UK356618 concentrations (Fig. 3E), strongly confirming MMP-3 responsiveness rather than hydrogel degradation as a dominating factor accounting for the on-demand pmTGF- β 1 release from the hydrogels.

3.4. *In vitro* chondrogenic capacity of the hydrogels

Gelatin was chosen as one of the main building components of the hydrogels due to the presence of RGD sequence in the structure for promoted cell adhesion and survival. To determine the biocompatibility of the β -CD-g-NHS/Ad- γ -ADH hydrogels, BMSCs were encapsulated within the hydrogels and cultured at 37 $^{\circ}$ C for one week. Live/dead cell

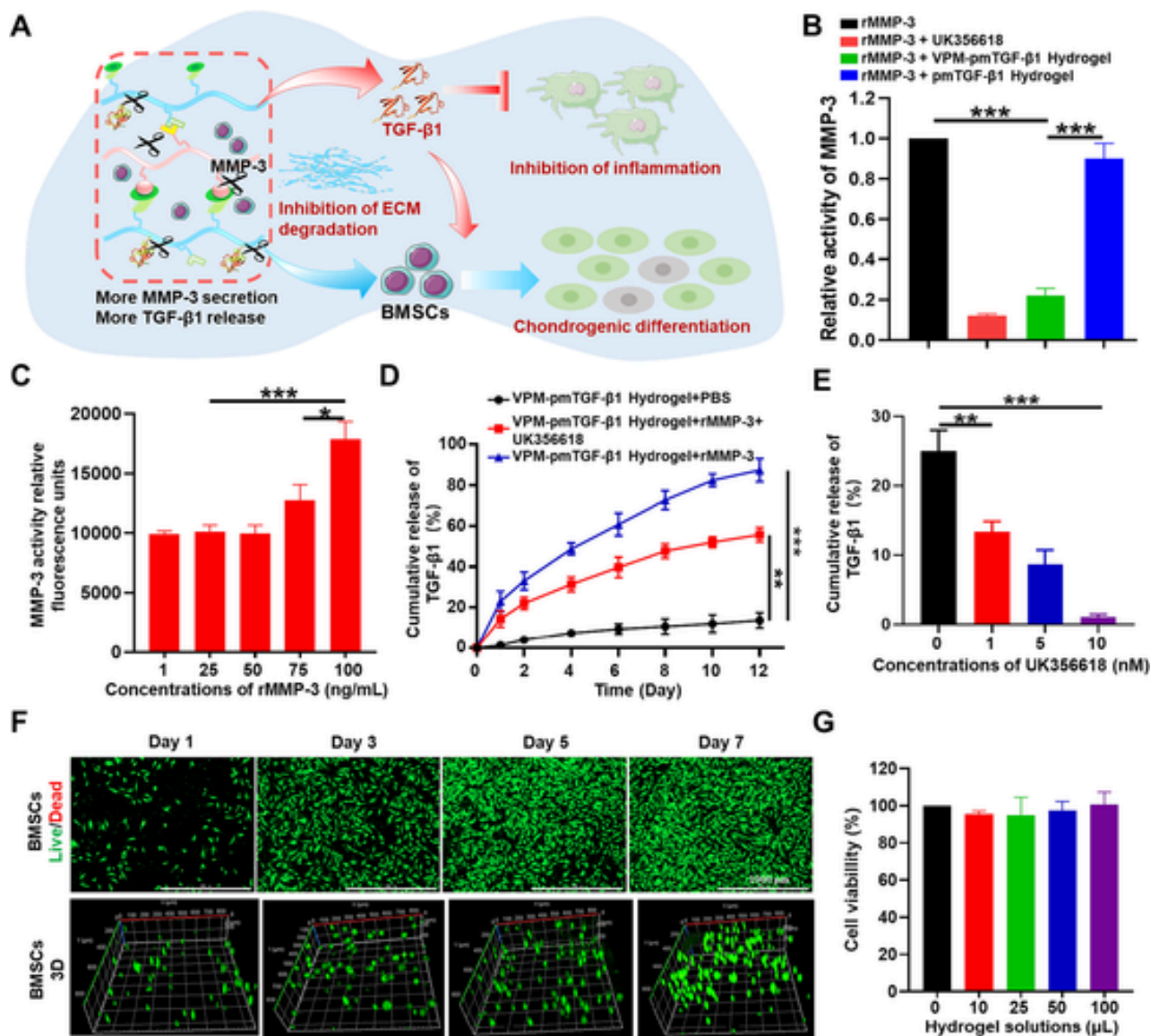


Fig. 3. In vitro studies of peptide release and biocompatibility of the β -CD-g-NHS/Ad-g-ADH hydrogels. (A) Schematic diagram of the VPM response to MMP-3 on-demand release of pmTGF- β 1, achieving the inhibition of MMP-3, suppression of inflammation and directed chondrogenic differentiation of BMSCs. (B) Analysis of the inhibition of MMP-3 activity by VPM-pmTGF- β 1 hydrogels. (C) Analysis of the inhibitory effect of the VPM-pmTGF- β 1 hydrogel on different MMP-3 concentrations. (D) Release behaviour of pmTGF- β 1 mediated by MMP-3 in response to different treatment groups. (E) Analysis of the dependence of the VPM-pmTGF- β 1 hydrogel response to MMP-3 on the UK356618 concentration. (F) Live/dead staining of the viability of BMSCs encapsulated in hydrogels and 3D culture images of BMSCs. Scale bar: 1000 μ m. (G) CCK-8 assays for the effect of hydrogel composition on the activity of BMSCs. (n = 4, *p < 0.05, **p < 0.01, and ***p < 0.001).

staining showed that BMSCs encapsulated on the hydrogels proliferated rapidly in the first 5 days, slowed down gradually from day 5 to day 7, and finally reached a plateau afterwards with an almost negligible number of dead cells (Fig. 3F). In addition, the effect of peptide-loaded hydrogel precursor solution amounts on chondrocyte activity was assessed using the CCK-8 assay, which indicated an insignificant effect of hydrogel solutions on the chondrocyte activity (Fig. 3G). Both results confirm the excellent biocompatibility and tolerability of the developed hydrogels for subsequent cellular and animal studies.

To investigate the potential of the hydrogel system to promote chondrogenesis, BMSCs were cultured in cartilage media containing 2 μ L of VPM-pmTGF- β 1 hydrogel solution, with daily changes of fresh medium for 21 days. Toluidine blue and H&E staining showed the appearance of cartilage tissue analogues for TGF- β 1 standard and VPM-pmTGF- β 1 hydrogel-treated pellets, suggesting the differentiation of a large number of BMSCs into chondrocytes (Fig. 4A). BMSCs were further mixed with

VPM-pmTGF- β 1 hydrogel precursor solution and cultured at 37 $^{\circ}$ C for 7 days, with rMMP-3 added to the media daily. Phalloidin (a cytoskeletal stain) staining confirmed a gradual morphological shift from an initial spindle shape of BMSCs to a polygonal shape of chondrocytes on day 7 of culture for the hydrogel-treated group (Fig. 4B).

BMSCs were also inoculated onto the hydrogel surface and cultured for 7 days with periodic media replacement. Alcian blue staining showed successful directed chondrogenic differentiation of BMSCs in the group treated with VPM-pmTGF- β 1 hydrogels in the presence of rMMP-3, as evidenced by the clear blue staining of acidic mucopolysaccharide in chondrocytes in contrast to those observed in the blank hydrogel group (Fig. 4C). To further confirm the chondrogenic differentiation of BMSCs in hydrogels, western blotting was used to identify chondrogenesis-related proteins. Aggrecan and Col II levels in BMSCs treated with TGF- β 1 standard or VPM-pmTGF- β 1 hydrogels were significantly higher than those of the PBS group and blank hydrogel group

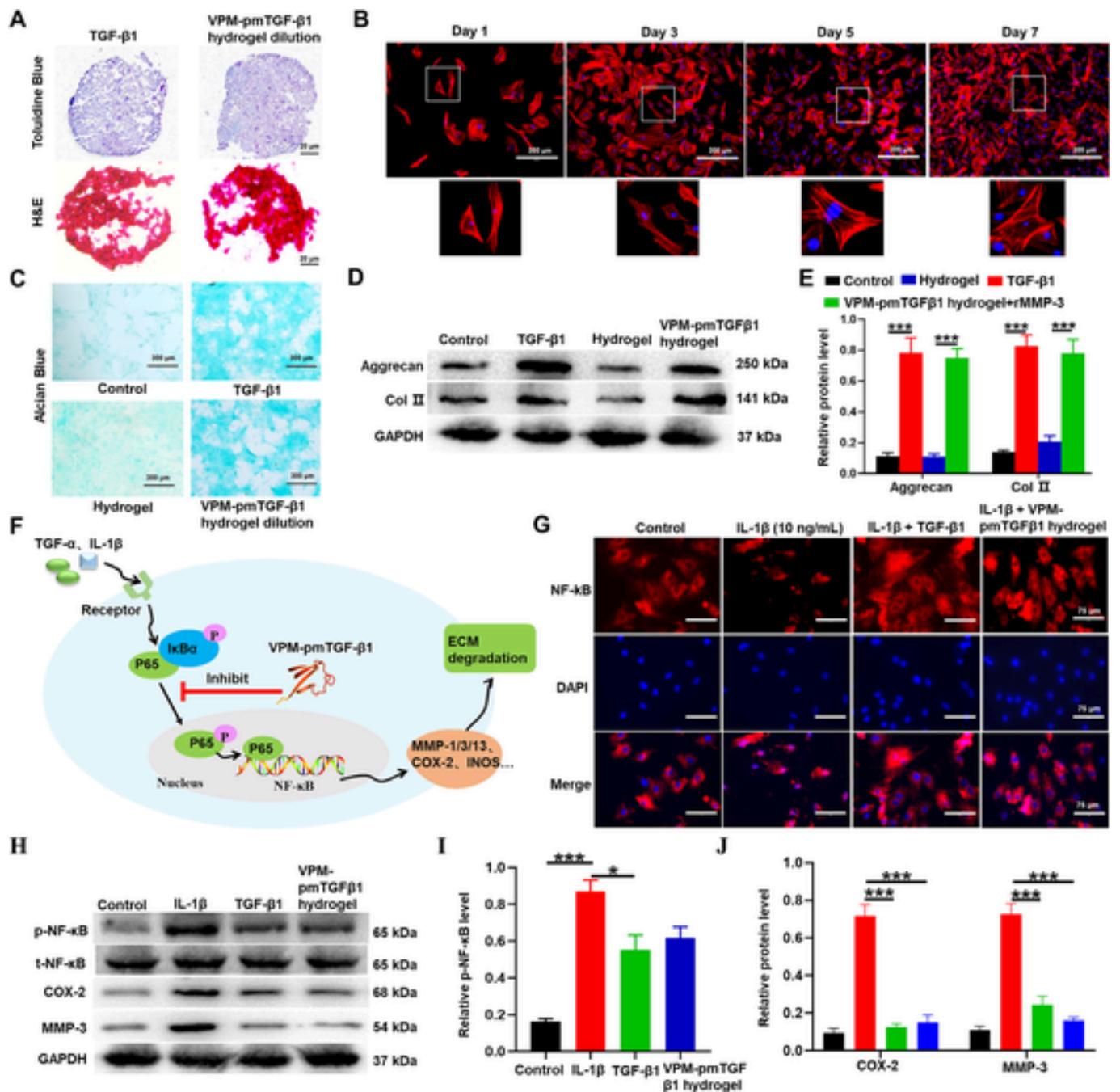


Fig. 4. In vitro effects of the hydrogels on the targeted cartilage differentiation of BMSCs and the inhibition of inflammation. (A) Toluidine blue and H&E staining to detect 3D cartilage differentiation of BMSCs. (B) Phalloidin staining of BMSCs cultured in VPM-TGF- β 1 hydrogels for 7 days. (C) Alcian blue staining of chondrogenic differentiation of BMSCs cultured in different treatment groups for 7 days. (D) Western blot analysis of the expression levels of Col II and aggrecan in BMSCs treated with different treatment groups. (E) Quantitative analysis of Col II and aggrecan expression levels. (F) Schematic representation of VPM-pmTGF- β 1 inhibition of NF- κ B nuclear translocation in chondrocytes. (G) Immunofluorescence detection of NF- κ B nuclear translocation in chondrocytes treated with different treatment groups. (H) Western blot analysis of the expression levels of total-NF- κ B (t-NF- κ B), phosphorylated-NF- κ B (p-NF- κ B), COX-2 and MMP-3 in chondrocytes treated with different treatment groups. (I, J) Quantitative analysis of the expression levels of t-NF- κ B, p-NF- κ B, COX-2 and MMP-3. (n = 3, *p < 0.05, **p < 0.01, and ***p < 0.001.). (For interpretation of the references to colour in this figure legend, the reader is referred to the web version of this article.)

(Fig. 4D, E), supporting the potential of the VPM-pmTGF- β 1 hydrogels to promote the targeted chondrogenic differentiation of BMSCs.

After cartilage injury, M1 macrophages release inflammatory factors, including TGF- α and IL-1 β , for rapid accumulation in the cartilage microenvironment. These factors can later bind to receptors on the surface of chondrocytes and activate the I κ B α /NF- κ B signaling pathway, leading to the NF- κ B nuclear translocation, initiating the cartilage damage program and ultimately the release of high levels of MMPs from

chondrocyte (Fig. 4F). To investigate the anti-inflammatory effect of VPM-pmTGF- β 1, IL-1 β (10 ng/mL) was used to induce an inflammatory response in chondrocytes. Immunofluorescence showed that IL-1 β induced NF- κ B nuclear translocation as nuclei colored with purple, whereas TGF- β 1 standard and VPM-pmTGF- β 1 inhibited NF- κ B nuclear translocation as nuclei colored with blue. The results suggested that VPM-pmTGF- β 1 inhibited the IL-1 β -induced chondrogenic degradation program (Fig. 4G). Western blot analysis further confirmed that the

VPM-pmTGF- β 1 hydrogels significantly reduced the expression of COX-2, MMP-3, and p-NF- κ B (p65) in chondrocytes (Fig. 4H-J). These findings validated that the VPM-pmTGF- β 1 hydrogels had anti-inflammatory effects similar to those of TGF- β 1 for repairing inflammatory damage in cartilage tissue.

3.5. In vivo inflammation regulation by the hydrogels

An important feature of the complex microenvironment after cartilage injury is the upregulated MMP-3 expression that remains low in uninjured normal tissues. The timeline for regeneration of damaged cartilage in SD rats by peptide-loaded hydrogels is shown in Fig. 5A. To determine the inhibitory effect of the VPM-pmTGF- β 1 hydrogel on MMP-3 in cartilage tissue, the hydrogel was injected into the injured cartilage using saline as a control. Western blot analysis revealed a downregulation of MMP-3, TGF- α , and IL-1 β expression levels starting after VPM-pmTGF- β 1 hydrogel treatment within one week and maintaining lower levels (Fig. 5B-E), likely due to the continual depletion of accumulated MMP-3 by VPM and subsequent pmTGF- β 1 release from the hydrogel in the cartilage for compromised MMP-3 and inflammatory factor levels. Western blot analyses of MMP-3 and inflammatory factors were further performed on all the rat cartilage on day 14. The VPM-pmTGF- β 1 hydrogel mediated the most significant downregulation of the MMP-3, TGF- α , and IL-1 β levels because VPM-pmTGF- β 1 can

undergo MMP-3-cleavable pmTGF- β 1 release dependent on MMP-3 levels (Fig. 5F-I). Further comparison of the MMP-3, TGF- α , and IL-1 β levels in the synovial fluid of injured cartilage on day 7 or day 14 revealed lower MMP-3, TGF- α , and IL-1 β levels for the BMSCs/VPM-pmTGF- β 1 hydrogel group than those of the saline group (Fig. S15), clearly indicating a sustained pmTGF- β 1 release in injured cartilage.

To better reflect the treatment effect in the cartilage defect area, immunofluorescence was used to detect M1 and M2 macrophages in the cartilage injury region of all groups at week 2. Immunofluorescence confirmed decreased proportions of CD86-labelled M1 macrophages and increased proportions of CD206-labelled M2 macrophages in the synovial tissues of rats treated with VPM-pmTGF- β 1 and BMSC/VPM-pmTGF- β 1 hydrogels compared with those of the other treatment groups, further suggesting a significant anti-inflammatory effect of the VPM-pmTGF- β 1 peptide sequence (Fig. 5J). Taken together, these results consistently confirmed that the VPM-pmTGF- β 1 hydrogel effectively inhibited inflammatory damage and promoted the repair of damaged cartilage by MMP-3-sensitive cleavage of VPM for on-demand pmTGF- β 1 release.

3.6. In vivo evaluation of cartilage regeneration by the hydrogels

To evaluate the in vivo cartilage regeneration potential of hydrogels, a full-thickness cartilage defect model was created in SD rats. After

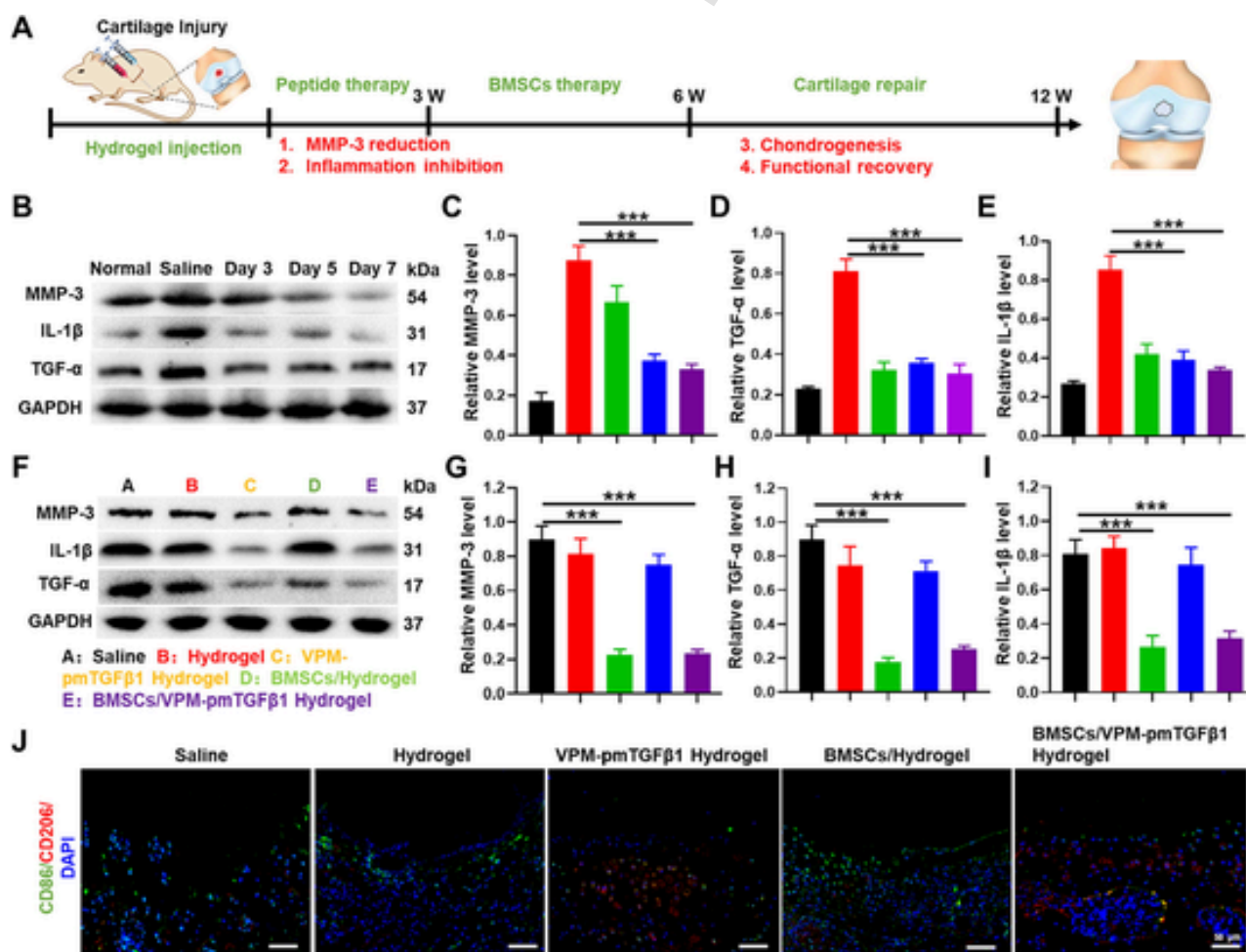


Fig. 5. In vivo studies of peptide release from the β -CD-g-NHS/Ad-g-ADH hydrogels. (A) Schematic diagram illustrating the surgical process and timetable for cartilage repair in SD rats. (B) Western blotting analysis of the effect of the VPM-TGF- β 1 hydrogel on the expression of MMP-3, IL-1 β , and TGF- α in cartilage tissues within one week. (C-E) Quantification of the expression levels of MMP-3, IL-1 β , and TGF- α from Fig. 5B. (F) Western blotting analysis of MMP-3, IL-1 β , and TGF- α expression levels in cartilage tissues of all groups on day 14. (G-I) Quantification of MMP-3, IL-1 β , and TGF- α expression levels from Fig. 5F. (J) Immunofluorescence detection of M1 (CD86) and M2 (CD206) macrophage levels in synovial tissue on day 14. (n = 3, *p < 0.05, **p < 0.01, and ***p < 0.001.).

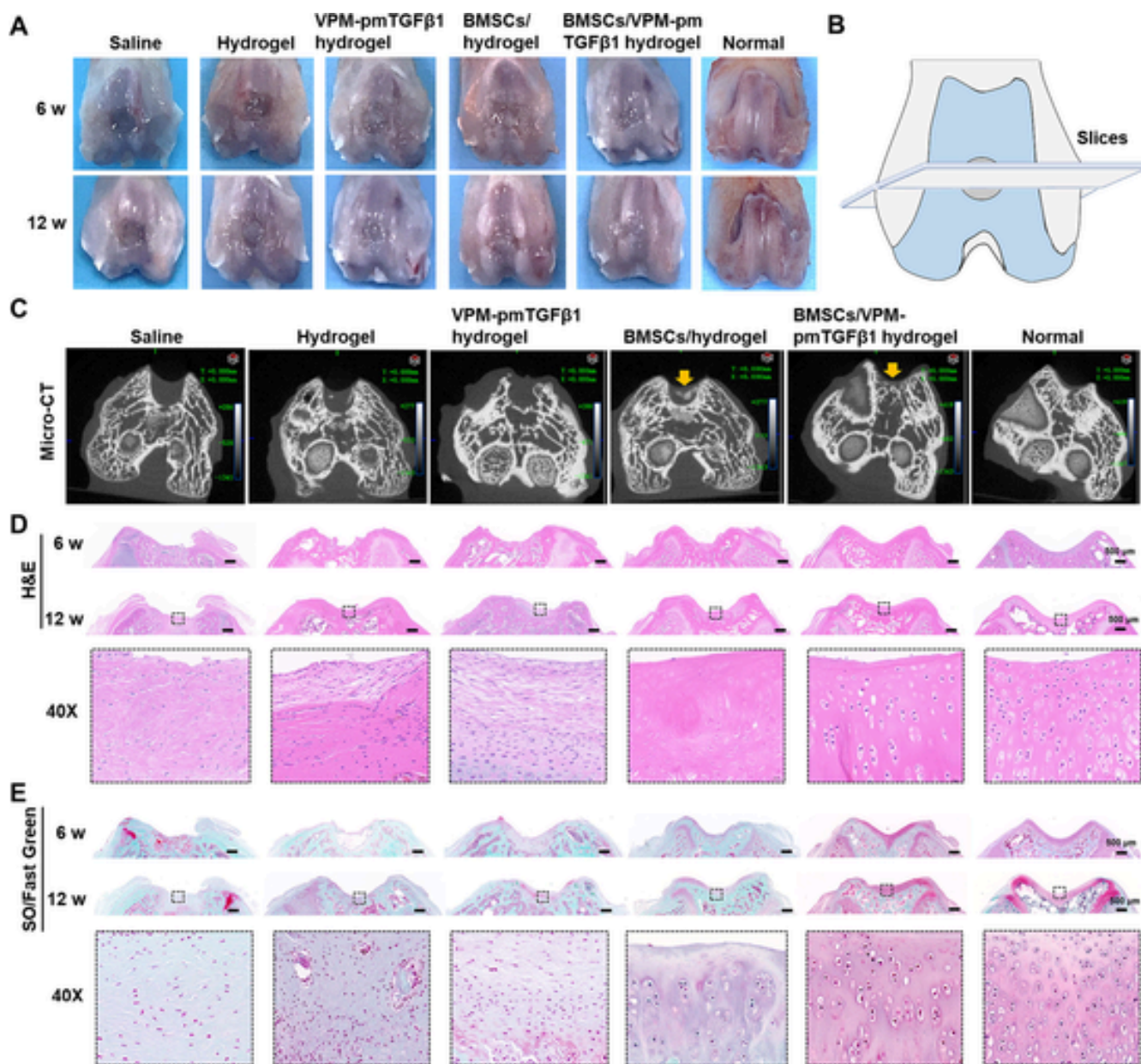


Fig. 6. In vivo cartilage regeneration in cartilage defects treated with different treatment groups. (A) Representative images of cartilage appearance in SD rats at 6- and 12-weeks post-treatment ($n = 5$). (B) Schematic diagram of cartilage slice location. (C) Micro-CT images showing 2D reconstruction of the repaired cartilage at 12 weeks after surgery. Yellow arrows indicate new cartilage generation. (D) Representative H&E-stained images of SD rat knee joints at 6 and 12 weeks. Scale bars: 500 μm . (E) Safranin O/Fast Green staining of SD rat knee joints at 6 and 12 weeks. Scale bars: 500 μm . (For interpretation of the references to colour in this figure legend, the reader is referred to the web version of this article.)

6 weeks of hydrogel implantation, the drilled defects were not completely covered by new cartilage tissue in all the groups. The border between the damaged region and the original cartilage was most obvious in the control group, whereas the new cartilage tissue formed in the BMSCs/VPM-TGF- β 1 hydrogel group was more tightly connected to the surrounding cartilage, probably due to the chondrogenic differentiation of BMSCs in the intrachondral environment, and the hydrogel improved the survival of BMSCs in the synovial fluid. After 12 weeks, the cartilage surface in the BMSCs/hydrogel group exhibited a relatively intact and hyaline cartilage-like tissue, whereas the surface in the saline group was not completely covered by new tissue and had poor cartilage regeneration (Fig. 6A). Notably, the BMSCs/VPM-TGF- β 1 hydrogel group exhibited intact new hyaline cartilage-like tissue with the best cartilage repair effect among all the groups. The cartilage tissue was then sectioned to further analyze the expression of newly regenerated cartilage

(Fig. 6B). Micro-CT showed that the BMSCs/hydrogel and BMSCs/VPM-pmTGF- β 1 hydrogel groups showed new cartilage generation in 12 weeks compared to those of the other groups with more significant formation of new cartilage in the BMSCs/VPM-pmTGF- β 1 hydrogel group (Fig. 6C). Further H&E and SO/Fast Green staining showed that the implanted BMSCs/VPM-pmTGF- β 1 hydrogel exhibited remarkable integration and newly regenerated hyaline cartilage-like tissue in 6 and 12 weeks (Fig. 6D, E). In contrast, the untreated group showed only a rough surface, minimal new tissue formation, and poor cartilage regeneration in 6 and 12 weeks. Although the VPM-pmTGF- β 1 hydrogel and BMSCs group both exhibited a small amount of new cartilage and bone tissue formation in 6 and 12 weeks, irregular fibrocartilage production was observed. Promisingly, the combination of BMSCs with VPM-pmTGF- β 1 hydrogel resulted in a smoother cartilage surface, extensive cartilage tissue generation, significant chondrocyte formation, and nice

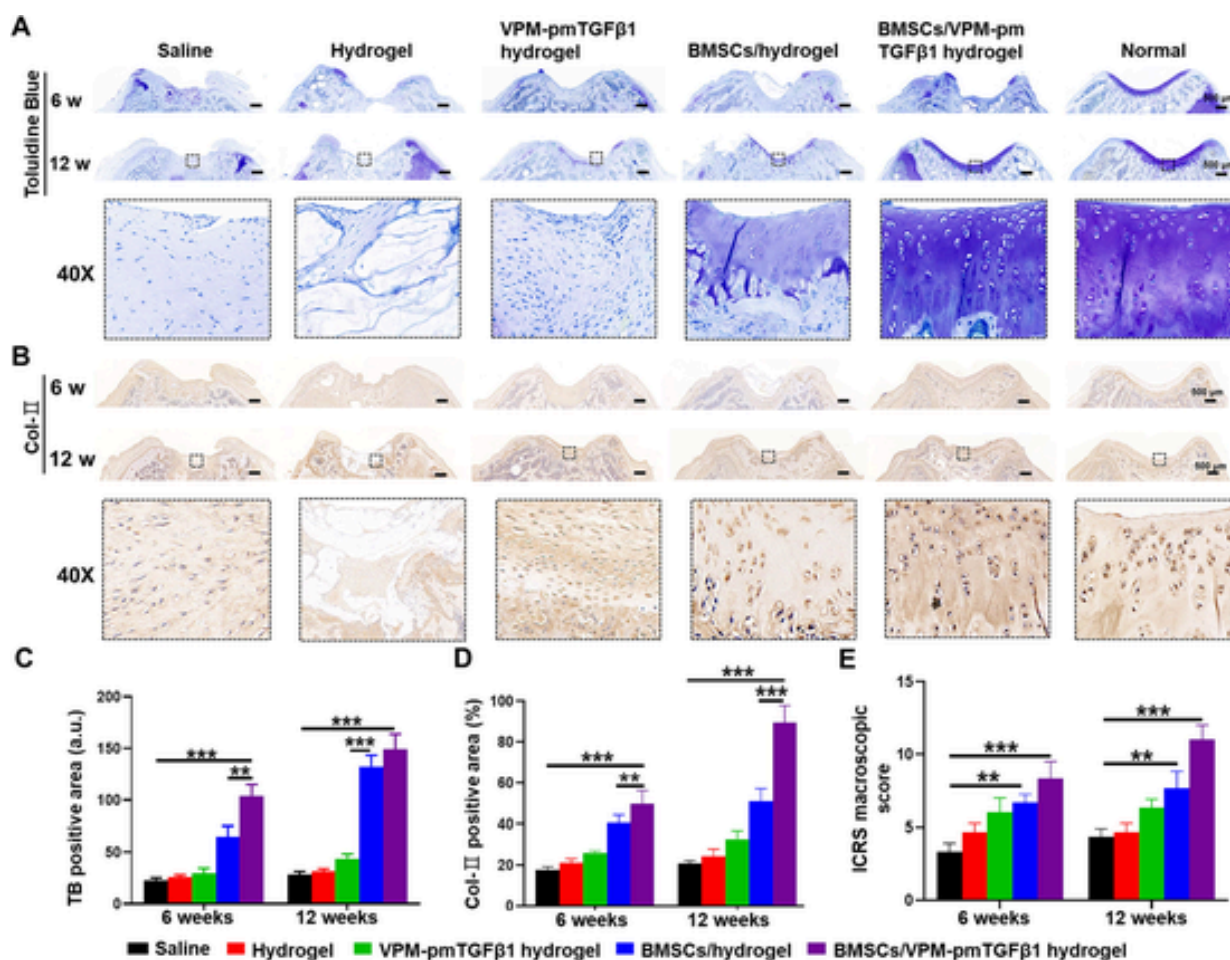


Fig. 7. Effect of different treatment groups on the expression of extracellular matrix proteins at cartilage defects. (A) Toluidine blue staining of cartilage at the defect in all groups (scale bar: 500 μm). (B) Immunohistochemical detection of cartilage collagen II expression in all groups (scale bar: 500 μm). (C) Quantification of ECM components (by toluidine blue staining). (D) Quantification of ECM components (by Col II immunostaining). (E) Results of ICRS macroscopic scores. All data are presented as the mean \pm SD. (n = 5, *p < 0.05, **p < 0.01, and ***p < 0.001.). (For interpretation of the references to colour in this figure legend, the reader is referred to the web version of this article.)

integration and orderly continuous structure formation between cartilage and subchondral bone.

Toluidine blue staining showed insignificant cartilage formation in the defect region of the saline group, whereas there was relatively good glycosaminoglycan (GAG) formation in the defect region of the BMSCs/hydrogel group. The GAG content in the BMSCs/VPM-pmTGF- β 1 hydrogel group was much higher than that of the BMSCs/hydrogel group, and the cartilage showed a well-integrated and ordered continuous structure between the cartilage and subchondral bone (Fig. 7A, C). Immunohistochemical analysis showed similar results, with higher expression of type II collagen and aggrecan in the regenerated cartilage tissue of the BMSCs/VPM-pmTGF- β 1 hydrogel group than those of the other groups (Fig. 7B, D). According to the International Cartilage Repair Society (ICRS) macroscopic scoring system, the regenerated cartilage in the saline group, blank hydrogel group, VPM-pmTGF- β 1 hydrogel group, BMSCs/hydrogel group and BMSCs/VPM-pmTGF- β 1 hydrogel group received scores of 3.6 ± 0.6 , 4.8 ± 1.1 , 5.9 ± 1.8 , 6.4 ± 0.9 and 8.3 ± 2.1 in 6 weeks, and 4.3 ± 0.8 , 5.5 ± 1.3 , 6.1 ± 1.5 , 7.3 ± 1.9 and 11.2 ± 1.8 in 12 weeks, respectively (Fig. 7E). The total score of the defects treated with the BMSCs/VPM-pmTGF- β 1 hydrogel was significantly higher than those of the other groups, strongly supporting the excellent performance of BMSCs/VPM-pmTGF- β 1 hydrogel in promoting cartilage regeneration, which thus can be used as a scaffold material for clinical cartilage regeneration.

Finally, the BMSCs/VPM-pmTGF- β 1 hydrogel had excellent biocompatibility, as reflected by the lack of significant differences in the expression levels of representative biochemical parameters of renal and hepatic function, including GGT, AST, ALP and ALT in all the groups (Fig. S16).

4. Conclusion

In summary, we have developed herein a peptide-based injectable hydrogel system for synergistic promoting the regeneration of damaged cartilage by integrating (i) a dual crosslinked network with excellent self-healing properties for shock absorption and lubrication, (ii) high water retention and stem cell adhesion abilities with strong affinity for cartilage matrix proteins to enhance three-dimensional cell-matrix interactions, (iii) an MMP-3-cleavable VPM peptide sequence to inhibit ECM degradation and achieve on-demand pmTGF- β 1 release for negative feedback regulation of the inflammatory process, and (iv) a pmTGF- β 1 peptide sequence to simultaneously promote targeted differentiation of BMSCs and efficient cartilage regeneration. Comprehensive in vitro and in vivo studies confirmed that this integrated therapeutic peptide-based hydrogel system provided a safe and effective solution for promoting cartilage regeneration, which could have a significant impact on the field of tissue engineering and regenerative medicine. Further studies are underway to explore the long-term efficacy and

safety of this strategy, but the acquired highly promising results definitely lay a strong foundation for upcoming studies in this area.

Declaration of Competing Interest

The authors declare that they have no known competing financial interests or personal relationships that could have appeared to influence the work reported in this paper.

Data availability

Data will be made available on request.

Acknowledgements

This work was supported by Hunan Science and Technology Innovation Leading Talent Project (2022RC3080), National Natural Science Foundation of China (81471777), Key R & D Program of Hunan Province (2021SK2036), post-doctoral funding from the University of South China (703,220XQD106), and Foundation of Hunan Provincial Natural Science Foundation of China (2023JJ40570).

Appendix A. Supplementary data

Supplementary data to this article can be found online at <https://doi.org/10.1016/j.cej.2023.145228>.

References

- J.L. Escobar Ivirico, M. Bhattacharjee, E. Kuyinu, L.S. Nair, C.T. Laurencin, Regenerative Engineering for Knee Osteoarthritis Treatment: Biomaterials and Cell-Based Technologies, *Engineering* 3 (1) (2017) 16–27.
- X. Yan, B. Yang, Y. Chen, Y. Song, J. Ye, Y. Pan, B. Zhou, Y. Wang, F. Mao, Y. Dong, D. Liu, J. Yu, Anti-Friction MSCs Delivery System Improves the Therapy for Severe Osteoarthritis, *Advanced materials* (Deerfield Beach, Fla.) 33 (52) (2021) e2104758.
- A. Hakamivala, L. Shuxin, K. Robinson, Y. Huang, S. Yu, B. Yuan, J. Borrelli Jr, L. Tang, Recruitment of endogenous progenitor cells by erythropoietin loaded particles for in situ cartilage regeneration, *Bioact Mater* 5 (1) (2020) 142–152, <https://doi.org/10.1016/j.bioactmat.2020.01.007>.
- X. Nie, Y.J. Chuah, W. Zhu, P. He, Y. Peck, D.A. Wang, Decellularized tissue engineered hyaline cartilage graft for articular cartilage repair, *Biomaterials* 235 (2020) 119821, <https://doi.org/10.1016/j.biomaterials.2020.119821>.
- Z. Zheng, C. Yu, H. Wei, Injectable Hydrogels as Three-Dimensional Network Reservoirs for Osteoporosis Treatment, *Tissue engineering, Part B, Reviews* 27 (5) (2021) 430–454, <https://doi.org/10.1089/ten.TEB.2020.0168>.
- S. Bai, M. Zhang, X. Huang, X. Zhang, C. Lu, J. Song, H. Yang, A bioinspired mineral-organic composite hydrogel as a self-healable and mechanically robust bone graft for promoting bone regeneration, *Chem. Eng. J.* 413 (2021) 127512.
- J. Gao, G. Zhang, K. Xu, D. Ma, L. Ren, J. Fan, J. Hou, J. Han, L. Zhang, Bone marrow mesenchymal stem cells improve bone erosion in collagen-induced arthritis by inhibiting osteoclast-related factors and differentiating into chondrocytes, *Stem Cell Res Ther* 11 (1) (2020) 171, <https://doi.org/10.1186/s13287-020-01684-w>.
- M.C. Embree, M. Chen, S. Pylawka, D. Kong, G.M. Iwaoka, I. Kalajzic, H. Yao, C. Shi, D. Sun, T.J. Sheu, D.A. Koslovsky, A. Koch, J.J. Mao, Exploiting endogenous fibrocartilage stem cells to regenerate cartilage and repair joint injury, *Nat. Commun.* 7 (2016) 13073, <https://doi.org/10.1038/ncomms13073>.
- M. Cai, X. Li, M. Xu, S. Zhou, L. Fan, J. Huang, C. Xiao, Y. Lee, B. Yang, L. Wang, R. William Crawford, Y. Xiao, L. Zhou, C. Ning, Y. Wang, Injectable Tumor Microenvironment-Modulated Hydrogels with Enhanced Chemosensitivity and Osteogenesis for Tumor-Associated Bone Defects Closed-Loop Management, *Chemical Engineering Journal* 450 (2022) 138086.
- M. Liu, X. Zeng, C. Ma, H. Yi, Z. Ali, X. Mou, S. Li, Y. Deng, N. He, Injectable hydrogels for cartilage and bone tissue engineering, *Bone Res* 5 (2017) 17014, <https://doi.org/10.1038/boneres.2017.14>.
- Z. Zheng, C. Lei, H. Liu, M. Jiang, Z. Zhou, Y. Zhao, C.Y. Yu, H. Wei, A ROS-Responsive Liposomal Composite Hydrogel Integrating Improved Mitochondrial Function and Pro-Angiogenesis for Efficient Treatment of Myocardial Infarction, *Adv. Healthc. Mater.* 11 (19) (2022) e2200990.
- S. Bernhard, M.W. Tibbitt, Supramolecular engineering of hydrogels for drug delivery, *Adv. Drug Deliv. Rev.* 171 (2021) 240–256, <https://doi.org/10.1016/j.addr.2021.02.002>.
- P. Li, Y. Zhong, X. Wang, J. Hao, Enzyme-Regulated Healable Polymeric Hydrogels, *ACS Cent. Sci.* 6 (9) (2020) 1507–1522, <https://doi.org/10.1021/acscentsci.0c00768>.
- G. Zhong, J. Yao, X. Huang, Y. Luo, M. Wang, J. Han, F. Chen, Y. Yu, Injectable ECM hydrogel for delivery of BMSCs enabled full-thickness meniscus repair in an orthotopic rat model, *Bioact Mater* 5 (4) (2020) 871–879, <https://doi.org/10.1016/j.bioactmat.2020.06.008>.
- Z. Zheng, Z. Guo, F. Zhong, B. Wang, L. Liu, W. Ma, C.Y. Yu, H. Wei, A dual crosslinked hydrogel-mediated integrated peptides and BMSC therapy for myocardial regeneration, *J. Control. Release* 347 (2022) 127–142, <https://doi.org/10.1016/j.jconrel.2022.04.010>.
- M.Y. Ha, D.H. Yang, S.J. You, H.J. Kim, H.J. Chun, In-situ forming injectable GFOGER-conjugated BMSCs-laden hydrogels for osteochondral regeneration, *NPJ Regen Med* 8 (1) (2023) 2, <https://doi.org/10.1038/s41536-022-00274-z>.
- Q. Feng, J. Xu, K. Zhang, H. Yao, N. Zheng, L. Zheng, J. Wang, K. Wei, X. Xiao, L. Qin, L. Bian, Dynamic and Cell-Infiltratable Hydrogels as Injectable Carrier of Therapeutic Cells and Drugs for Treating Challenging Bone Defects, *ACS Cent. Sci.* 5 (3) (2019) 440–450, <https://doi.org/10.1021/acscentsci.8b00764>.
- W. Shi, M. Sun, X. Hu, B.o. Ren, J. Cheng, C. Li, X. Duan, X. Fu, J. Zhang, H. Chen, Y. Ao, Structurally and Functionally Optimized Silk-Fibroin-Gelatin Scaffold Using 3D Printing to Repair Cartilage Injury In Vitro and In Vivo, *Advanced materials* (Deerfield Beach, Fla.) 29 (29) (2017) 1701089.
- H. Kwon, W.E. Brown, C.A. Lee, D. Wang, N. Paschos, J.C. Hu, K.A. Athanasiou, Surgical and tissue engineering strategies for articular cartilage and meniscus repair, *Nat. Rev. Rheumatol.* 15 (9) (2019) 550–570, <https://doi.org/10.1038/s41584-019-0255-1>.
- C. Garcia Garcia, S.S. Patkar, B. Wang, R. Abouomar, K.L. Kiick, Recombinant protein-based injectable materials for biomedical applications, *Adv. Drug Deliv. Rev.* 193 (2023) 114673.
- C.P. Ting, M.A. Funk, S.L. Halaby, Z. Zhang, T. Gonen, W.A. van der Donk, Use of a scaffold peptide in the biosynthesis of amino acid-derived natural products, *Science* 365 (6450) (2019) 280–284.
- D. Liu, M. Nikoo, G. Boran, P. Zhou, J.M. Regenstein, Collagen and gelatin, *Annu Rev. Food, Sci Technol* 6 (2015) 527–557, <https://doi.org/10.1146/annurev-food-031414-111800>.
- H.A. Awad, M.Q. Wickham, H.A. Leddy, J.M. Gimble, F. Guilak, Chondrogenic differentiation of adipose-derived adult stem cells in agarose, alginate, and gelatin scaffolds, *Biomaterials* 25 (16) (2004) 3211–3222, <https://doi.org/10.1016/j.biomaterials.2003.10.045>.
- L. Gong, J. Li, J. Zhang, Z. Pan, Y. Liu, F. Zhou, Y. Hong, Y. Hu, Y. Gu, H. Ouyang, X. Zou, S. Zhang, An interleukin-4-loaded bi-layer 3D printed scaffold promotes osteochondral regeneration, *Acta Biomater.* 117 (2020) 246–260, <https://doi.org/10.1016/j.actbio.2020.09.039>.
- M. Cao, J. Feng, S. Sirisansaneeyakul, C. Song, Y. Chisti, Genetic and metabolic engineering for microbial production of poly- γ -glutamic acid, *Biotechnol. Adv.* 36 (5) (2018) 1424–1433, <https://doi.org/10.1016/j.biotechadv.2018.05.006>.
- X. Liu, S. Liu, R. Yang, P. Wang, W. Zhang, X. Tan, Y. Ren, B. Chi, Gradient chondroitin sulfate/poly (γ -glutamic acid) hydrogels inducing differentiation of stem cells for cartilage tissue engineering, *Carbohydr. Polym.* 270 (2021) 118330, <https://doi.org/10.1016/j.carbpol.2021.118330>.
- Y. Tan, H. Huang, D.C. Ayers, J. Song, Modulating Viscoelasticity, Stiffness, and Degradation of Synthetic Cellular Niches via Stoichiometric Tuning of Covalent versus Dynamic Noncovalent Cross-Linking, *ACS central science* 4 (8) (2018) 971–981, <https://doi.org/10.1021/acscentsci.8b00170>.
- M. Dai, B. Sui, Y. Hua, Y. Zhang, B. Bao, Q. Lin, X. Liu, L. Zhu, J. Sun, A well defect-suitable and high-strength biomimetic squid type II gelatin hydrogel promoted in situ costal cartilage regeneration via dynamic immunomodulation and direct induction manners, *Biomaterials* 240 (2020) 119841, <https://doi.org/10.1016/j.biomaterials.2020.119841>.
- T.P.T. Nguyen, F. Li, S. Shrestha, R.S. Tuan, H. Thissen, J.S. Forsythe, J.E. Frith, Cell-laden injectable microgels: Current status and future prospects for cartilage regeneration, *Biomaterials* 279 (2021) 121214, <https://doi.org/10.1016/j.biomaterials.2021.121214>.
- L.D. Halder, E.A.H. Jo, M.Z. Hasan, M. Ferreira-Gomes, T. Krüger, M. Westermann, D.I. Palme, G. Rambach, N. Beyersdorf, C. Speth, I.D. Jacobsen, O. Kniemeyer, B. Jungnickel, P.F. Zipfel, C. Skerka, Immune modulation by complement receptor 3-dependent human monocyte TGF- β 1-transporting vesicles, *Nat. Commun.* 11 (1) (2020) 2331, <https://doi.org/10.1038/s41467-020-16241-5>.
- J. Li, J. Wang, Y. Zou, Y. Zhang, D. Long, L. Lei, L. Tan, R. Ye, X. Wang, Z. Zhao, The influence of delayed compressive stress on TGF- β 1-induced chondrogenic differentiation of rat BMSCs through Smad-dependent and Smad-independent pathways, *Biomaterials* 33 (33) (2012) 8395–8405, <https://doi.org/10.1016/j.biomaterials.2012.08.019>.
- J. Maihöfer, H. Madry, A. Rey-Rico, J.K. Venkatesan, L. Goebel, G. Schmitt, S. Speicher-Mentges, X. Cai, W. Meng, D. Zurakowski, M.D. Menger, M.W. Laschke, M. Cucchiari, Hydrogel-Guided, rAAV-Mediated IGF-I Overexpression Enables Long-Term Cartilage Repair and Protection against Perifocal Osteoarthritis in a Large-Animal Full-Thickness Chondral Defect Model at One Year In Vivo, *Advanced materials* (Deerfield Beach, Fla.) 33 (16) (2021) e2008451.
- D.J. Leong, X.I. Gu, Y. Li, J.Y. Lee, D.M. Laudier, R.J. Majeska, M.B. Schaffler, L. Cardoso, H.B. Sun, Matrix metalloproteinase-3 in articular cartilage is upregulated by joint immobilization and suppressed by passive joint motion, *Matrix Biol* 29 (5) (2010) 420–426, <https://doi.org/10.1016/j.matbio.2010.02.004>.
- A. Lerner, S. Neidhöfer, S. Reuter, T. Matthias, MMP3 is a reliable marker for disease activity, radiological monitoring, disease outcome predictability, and therapeutic response in rheumatoid arthritis, *Best Pract Res Clin Rheumatol* 32 (4) (2018) 550–562, <https://doi.org/10.1016/j.berh.2019.01.006>.
- E. Sugiyama, Role of matrix metalloproteinase-3 in joint destruction in rheumatoid arthritis, *Clin. Calcium* 17 (4) (2007) 528–534.
- L. Lin, R.E. Marchant, J. Zhu, K. Kottke-Marchant, Extracellular matrix-mimetic

- poly(ethylene glycol) hydrogels engineered to regulate smooth muscle cell proliferation in 3-D, *Acta Biomater.* 10 (12) (2014) 5106–5115, <https://doi.org/10.1016/j.actbio.2014.08.025>.
- [37] X. Ding, J. Gao, X. Yu, J. Shi, J. Chen, L. Yu, S. Chen, J. Ding, 3D-Printed Porous Scaffolds of Hydrogels Modified with TGF- β 1 Binding Peptides to Promote In Vivo Cartilage Regeneration and Animal Gait Restoration, *ACS Appl. Mater. Interfaces* 14 (14) (2022) 15982–15995, <https://doi.org/10.1021/acsami.2c00761>.
- [38] Q. Wei, D. Liu, G. Chu, Q. Yu, Z. Liu, J. Li, Q. Meng, W. Wang, F. Han, B. Li, TGF- β 1-supplemented decellularized annulus fibrosus matrix hydrogels promote annulus fibrosus repair, *Bioact Mater* 19 (2023) 581–593, <https://doi.org/10.1016/j.bioactmat.2022.04.025>.
- [39] Y. Han, B. Jia, M. Lian, B. Sun, Q. Wu, B. Sun, Z. Qiao, K. Dai, High-precision, gelatin-based, hybrid, bilayer scaffolds using melt electro-writing to repair cartilage injury, *Bioact Mater* 6 (7) (2021) 2173–2186, <https://doi.org/10.1016/j.bioactmat.2020.12.018>.
- [40] Q. Zhou, Y. Cai, Y. Jiang, X. Lin, Exosomes in osteoarthritis and cartilage injury: advanced development and potential therapeutic strategies, *Int. J. Biol. Sci.* 16 (11) (2020) 1811–1820, <https://doi.org/10.7150/ijbs.41637>.
- [41] A.R. Armiento, M. Alini, M.J. Stoddart, Articular fibrocartilage - Why does hyaline cartilage fail to repair? *Adv. Drug Deliv. Rev.* 146 (2019) 289–305, <https://doi.org/10.1016/j.addr.2018.12.015>.
- [42] P. Bertsch, M. Diba, D.J. Mooney, S.C.G. Leeuwenburgh, Self-Healing Injectable Hydrogels for Tissue Regeneration, *Chem. Rev.* 123 (2) (2023) 834–873, <https://doi.org/10.1021/acs.chemrev.2c00179>.
- [43] T. Hamada, N. Arima, M. Shindo, K. Sugama, Y. Sasaguri, Suppression of adjuvant arthritis of rats by a novel matrix metalloproteinase-inhibitor, *Br J Pharmacol* 131 (8) (2000) 1513–1520, <https://doi.org/10.1038/sj.bjp.0703751>.
- [44] B.J. Kang, J. Ryu, C.J. Lee, S.C. Hwang, Luteolin Inhibits the Activity, Secretion and Gene Expression of MMP-3 in Cultured Articular Chondrocytes and Production of MMP-3 in the Rat Knee, *Biomol Ther (Seoul)* 22 (3) (2014) 239–245, <https://doi.org/10.4062/biomolther.2014.020>.
- [45] W. Hui, G.J. Litherland, M.S. Elias, G.I. Kitson, T.E. Cawston, A.D. Rowan, D.A. Young, Leptin produced by joint white adipose tissue induces cartilage degradation via upregulation and activation of matrix metalloproteinases, *Ann. Rheum. Dis.* 71 (3) (2012) 455–462, <https://doi.org/10.1136/annrheumdis-2011-200372>.
- [46] J. Wei, P. Ran, Q. Li, J. Lu, L. Zhao, Y. Liu, X. Li, Hierarchically structured injectable hydrogels with loaded cell spheroids for cartilage repairing and osteoarthritis treatment, *Chem. Eng. J.* 430 (2022) 132211.